SPE-195964-MS

Permanent Storage of CO_2 in Mexican Igneous Rocks

Erick Cantú-Apodaca, Pilar Ortiz-Lucas, Ana Paulina Gómora-Figueroa, Javier Mancera-Alejández, and Enrique González-Torres, UNAM

This paper was prepared for presentation at the SPE Annual Technical Conference and Exhibition held in Calgary, Alberta, Canada, 30 Sep - 2 October 2019.

Abstract

Mexico has undertaken a series of measures to implement Carbon Capture and Storage (CCS) technology due to the acquired national and international commitments regarding the reduction of GHG emissions as well as their implications to climate change. So far, the screening of the different methods for geological storage of CO_2 potentially applicable in Mexico includes deep saline aquifers, non-economic coal beds, and crude oil reservoirs for EOR.

Storage of carbon dioxide projects in igneous rocks has been successful in the past. According to the literature, there are about eight sites, onshore, in the world with plenty of igneous rocks to store CO_2, and Mexico is one of these sites. However, little attention has been paid to the study of igneous rocks as a potential method for geological storage of carbon dioxide.

This work aims the first petrographic and geochemical analysis to estimate the feasibility of CO_2 mineralization thorough Mexican basaltic formations. This analysis includes the identification of the main CO_2 emission areas in Mexico, the collection of samples near to large CO_2 emissions sites and, the characterization of the samples by different tests and techniques. The properties of the rock samples and water were studied after the tests to compare changes in mineral phases and water composition.

The results herein confirm the feasibility of Mexican basalts to react in the presence of CO_2 but also set the recommendations for the next steps to take to determine the technical feasibility of the CO_2 permanent storage using basalts in Mexico.

Introduction

With the rise in global population during the last decades, the use of transport, garbage generation, agricultural and industry activities, had led to a drastic increase of the energy consumption, triggering a considerable growth in greenhouse gas emissions (GHG). On average, carbon dioxide (CO_2) represents 60% of the greenhouse gases emissions, while in some countries it represents over 80%.[1]

In the particular case of Mexico, the GHG emissions in carbon dioxide equivalent units (CO_{2eq}) grew 33% by 2010 in comparison with 1990, giving a total of 748 million tons $CO_{2eq.}$[2] The principal emitted GHG, is CO_2 (80.4%), followed by CH_4 (16.9%) and N_2O (2.7%).[2] Since 2008, Mexico has undertaken a series measures to implement CCS technology due to the acquired national and international commitments

regarding the energy supply, clean energy usage, and the reduction of GHG emissions and their implications to climate change.[3 4] So far, the screening of the different methods for geological storage of CO_2 potentially applicable in Mexico includes deep saline aquifers, non-economic coal beds, and crude oil reservoirs for EOR. However, little attention has been paid to the study of igneous rocks as a potential method for geological storage of carbon dioxide.

Permanent storage of CO_2 in igneous rocks is feasible and has been proven by the CarbFix project in Iceland, which its pilot phase ran for over decade and consisted of creating the basis for the fixation of carbon dioxide in the subsurface through the in-situ carbonation of basalts, and the demonstration of this technology by fixing approximately 200 tons of injected CO_2 as carbonate minerals during 2012 and 2013. The results of the tests indicate that about 90% of the injected CO_2 was mineralized in less than a year, without any gas leakage detected.[5] Rather than re-injecting CO_2 directly into a geological formation, the CarbFix project dissolves the gas stream into formation fluids and well water during injection. This solubility-trapping approach promotes carbonation of the basalt and long-term storage of CO_2. The rate of mineralization depends on the mineral composition of the basalts and the rate at which divalent cations (Ca^{2+}, Mg^{2+}, and Fe^{3+}) are released from silicate minerals.[6]

About 5% of the continents and most of the oceanic floor are comprised of basaltic rocks, including the mid-oceanic ridges.[7] The largest basaltic storage potential lies offshore; theoretically all CO_2 from the burning of fossil fuel carbon (~5,000 Gt)[7] could be stored by mineral carbonation along the mid-ocean ridges.[8 9] While onshore, for example, the Columbia River basalts in the USA have a volume in excess of 200,000 km^3 and the Siberian basalts have a volume higher than 1,000,000 km^3. These large volumes have correspondingly large CO_2 sequestration capacities: estimated that the Columbia River basalts alone can sequester over 100Gt of CO_2.[10]

On the other hand, the Trans-Mexican Volcanic Belt (TMVB) is a 1,000 km long Neogene continental arc showing a significant variation in composition and volcanic style, and intra-arc extensional tectonics. It overlies the Rivera and Cocos slabs, which display marked changes in geometry and the fluids from the slab are released in a 40 to 100 km wide belt beneath the frontal part of the arc.[11] According to the literature, TMVB is one of the most abundant places with the presence of basaltic and andesitic rocks.[12] However, additional information regarding the total volume of basaltic rock in the TMVB, including the subsurface, is limited (see Table 2 and Figure 2).

The goal of this work consists of the petrographic and geochemical analysis to estimate the feasibility of CO_2 mineralization into sedimentary rocks, through the injection of CO_2 into Mexican basaltic formations. To achieve this goal, the following activities were followed: a) identification of the main CO_2 emission areas in Mexico, b) collection of samples close to these large CO_2 emissions sites and, c) analysis of the samples by X-ray powder diffraction, X-ray fluorescence, infrared spectroscopy, and petrographic analysis. The best candidates were used for fixed and continuous CO_2 laboratory tests under different conditions. The properties of the rock samples and water were studied after the tests to compare changes in mineral phases and water composition.

Background

Geological storage relies on the injection of CO_2 into porous rock formations, involving sedimentary basins, depleted oil reservoirs, and non-economic coal beds. Impermeable cap rock is essential because CO_2 density is less than that of the water, so buoyancy tends to drive CO_2 upwards, back to the surface. Several industrial-scale geologic CO_2 storage programs are already underway, including the Norwegian Sleipner project in the North Sea and the Weyburn project in Canada. At these sites, a million tons of CO_2 is injected into the subsurface each year. Despite the large annual injected volume, these projects, and other similar efforts, currently store less than 0.01%, of the global annual anthropogenic CO_2 production.[13]

According to the Global Carbon Atlas[14] in 2017, Mexico was in the Top 20 CO_2-emitting countries ranked in the 11th position (490 $MtCO_2$). To address GHG emissions and their implications, it is mandatory to explore all the methods with potential for CO_2 storage and sequestration.

Since CarbFix demonstrated how interdisciplinary collaboration allowed a fast and efficient development on how to permanently storage CO_2 in subsurface basalt formations by mineralization of this gas, meaning the fixation of CO_2 as stable carbonate minerals, such as calcite ($CaCO_3$), dolomite ($Ca_{0.5}Mg_{0.5}CO_3$), magnesite ($MgCO_3$) and siderite ($FeCO_3$).[15]

In particular, to consider Mexican basaltic rocks of TMVB as a prospective method for CO_2 geological storage, it is necessary to understand their characteristics and petrogenesis, as well as to looking into to the possible similarities and differences between the basalt rocks from Iceland and Mexico to estimate Mexico's potential. Table 1 shows the main characteristics of the TMVB and Iceland basalt plateau.

Table 1—Most relevant characteristics of Trans-Mexican Volcanic Belt (TMVB) and the Iceland Basalt Plateau.

Mexico (TMVB)[11 16]	Iceland[8]
• It is a continental magmatic arc, constituted by about 8,000 volcanic structures and some intrusive bodies. The province is approximately 1,000 km long and has an irregular amplitude between 80 and 230 km. • The TMVB is built over a heterogenic continental crust basement, in lithology and ages that go from the Proterozoic to the Triassic, factor that influences on the geochemical diversity arc. • Four compositional groups: Alkaline-sodium rocks, alkaline-potassium rocks, calcialcaline rocks and rhyolitic volcanism. • Rocks with subalkaline (83% of the analyzes), while alkaline rocks are presented in a subordinate way. In the classification scheme of LeMaitre (1989), the vast majority of subalkaline rocks belong to the calc-alkaline series with average K content (~ 86% of the analyzes), while calc-alkaline rocks rich in K are less abundant. • Alkaline rocks can be divided into sodium and potassium using the diagram of Le Bas et al, 1986. In this case, alkaline sodium rocks are relatively more abundant (62% of the analyzes). • The composition of major elements is significantly different in the three types of rocks. Alkaline rocks tend to show SiO_2 concentrations of less than 60%, and the TiO_2 and P_2O_5 contents reach the highest values. • Most of the subalkaline rocks have low values of Nb (<20 ppm), although some samples reach values up to 40 ppm and the high contents of the rhyolitic rocks are notorious. In contrast, potassium alkaline rocks are characterized by very high contents of Sr (up to 5.109 ppm) and Ba (up to 4.765 ppm), while alkaline sodium rocks may have values only slightly higher than subalkaline rocks.	• The Iceland basalt plateau rises more than 3,000 m above the surrounding sea floor and covers about 350,000 km^2. Iceland itself is 103,000 km^2, mostly made of young 0-20 M yr. igneous rocks and sediments thereof. • The target CO_2 storage formation was at between 400 and 800 m depth and consists of basaltic lavas and hyaloclastites with lateral and vertical intrinsic permeabilities of 300 and 1700 ×10–15 m^2, respectively. • The subsurface rocks at the injection site are primarily olivine tholeiite basalts, consisting of post-glacial lava flows and glassy hyaloclastite formations, formed beneath the ice-sheet during glaciations. The bedrock down to about 200–300 m depth consists of relatively unaltered olivine tholeiite lava flows that host an oxygen-rich groundwater system with a static water table at about 100 m depth. Below the lava flows lies a 200 m thick, slightly altered hyaloclastite that separates the near surface water system from a deeper system, which is oxy-gen depleted. • The most abundant alteration minerals from 200 m to 1,000 m depth are smectites, calcite, and Ca-and Na-rich zeolites.[8]

The alkaline volcanism of the TMVB is complex and varied; in the western sector, there is bimodal volcanism with dacito-rhyolitic domes and monogenetic basaltic and basaltic-andesitic centers. In the central sector, there are small shield volcanoes and monogenetic centers of basaltic or basalt-andesitic composition. In the eastern sector, the volcanism is located in large stratovolcanoes, calderas, and dome-complexes of andesitic to the rhyolitic composition that is aligned with cortical structures and to a lesser extent monogenetic collars of basalt composition.[16 17] Only some of the alkaline rocks can be interpreted as oceanic island basalts (OIB).[11]

Regarding the differences between the mafic volcanic rocks from the TMVB and those from Iceland, the tectonic environment is one of them. While in Iceland there is an oceanic ridge that produces slightly differentiated magmas, in the TMVB, the magmatism is associated with the subduction of the Rivera and Cocos Plates, underneath the North American Plate. Therefore, the generated magmas show a higher spectrum of differentiation.

The volcanic rocks of Iceland exhibit regular forms of great extension and more uniform thicknesses, unlike the Mexican basalts, which are limited in lateral extension since they occur in a great diversity of volcanic structures, such as stratovolcanoes, domes, calderas, among others. Besides the volcanic products fill up irregular reliefs; thus, their thicknesses show more significant variation. Nevertheless, in the northwestern sector of the TMVB, voluminous manifestations of basaltic flows[18] have been described, which could be of interest for CO_2 mineralization due to their size.

Identification of the main CO_2 emission areas in Mexico

It was necessary to identify the areas exhibiting the most significant CO_2 emissions in Mexico to identify the best place for the collection of samples in this study. The route map published in 2014[3] gathered the principal fixed sources of carbon dioxide in the country (Figure 1), where electricity generation (blue), cement production (orange) and oil, gas, and petrochemical industry (red) represent the most significant CO_2 emission points. It is worth to mention that Mexico is a water-stressed country;[19] therefore, water extensive-use technologies must preferably be applied close to water sources such the oceans, where the water supply for human consumption do not compete with the technology to implement. Figure 1 exhibits that the activities in Mexico producing higher CO_2 emissions are located in the North and Southeast of the country. For this study we focus on the Southeast region of Mexico for three reasons: 1) the highest anthropogenic CO_2 emissions in the country are produced in this section, 2) the Trans-Mexican Volcanic Belt is near to the fixed CO_2 sources (Figure 2) and, 3) the Gulf of Mexico, a source of water, for CCS technology is close to this area; consequently, no human water sources are compromised if this sort of technology is to be applied in Mexico.

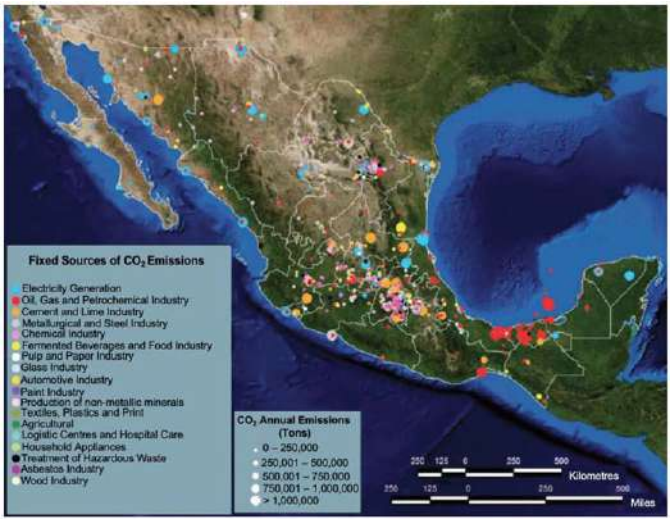

Figure 1—Principal fixed sources of GHG emissions in Mexico. Modified from *"Atlas de almacenamiento geológico de CO_2 México, SENER-CFE"*.[20]

Collection and Characterization of Samples

In addition to the identification of the main CO_2 emission areas in Mexico it is necessary to mention that in the TMVB there are important extensions of exposed basaltic rocks, however, three zones exhibit significant potential for CO_2 storage due to their volume and geochemical composition (Table 2).

Table 2—Zones with potential for CO2 storage in the TMVB,[21] figure 2, shows the approximate location of each zone.

Zone	Location	Exposed area	General features
1	NE of Guadalajara, Altos de Jalisco region	At least 6,000 km^2	Late Miocene to early Pliocene. Balsaltic lava flows and cinder cones
2	Surroundings of Querétaro City	Approximately 670 km^2	Late Miocene to early Pliocene. Balsaltic lava flows and cinder cones
3	Tlaxcala-Puebla	131 km^2 Tlaxco 265 km^2 Disperse outcrops between Sahagun City and Tulancingo	Late Pliocene to Quaternary. Monogenetic cones and associated lava flows

Since previous studies of the Mexican basaltic rocks are surficial, the depth and the lateral variations of these rocks are unknown. Therefore, it is essential to develop more detailed cartography of the zones exhibiting the most promising properties for CO_2 storage. Also, is necessary perform drilling activities for recovering and logging cores, as well as to develop geophysical exploration to identify the thickness, and spatial distribution of basalts to estimate the rock volume for zones 1, 2 and 3 (see Figure 2).

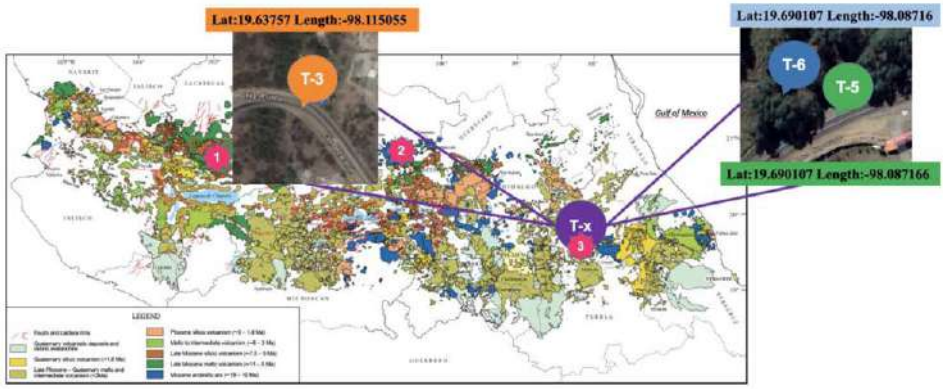

Figure 2—The red stars 1, 2 and 3 represent the zones with more significant potential in Mexico for CO_2 storage. The collected samples, T-01 to T-07 (T-x), for this study are from; a) Mafic volcanism to the middles Pliocene of the Late Quaternary and b) Andesitic volcanic arc of the Miocene. These formations are located between the states of Puebla, Tlaxcala and Hidalgo. T-03, T-05 and T-06 were selected due to its properties for CO_2 injection experiments.

Seven different samples (T-01 to T-07) were collected from: a) Mafic volcanism to the middles Pliocene of the Late Quaternary (<3My) and b) Andesitic volcanic arc of the Miocene (~19- 10 My). These formations are located between the states of Puebla, Tlaxcala and Hidalgo. As shown in the following sections, samples T-03, T-05, and T-06 were selected due to its properties for CO_2 injection experiments. T-03, was collected in; Length: 98 ° 06'54.2" W, Latitude: 19 ° 38'15.2" N (Length: −98.115055 and Latitude: 19.63757); T-05 and T-06 were collected in: Length: 98 ° 05'13.8" W, Latitude: 19 ° 41'24.4" N (Length: −98.087166 and Latitude: 19.690107), see Figure 2.

The basaltic rocks were crushed using a cotton towel and a hammer. The fine particles were removed, later smaller samples were brushed to remove rock powder, and cleaned with cycles of distilled water and then isopropanol. The remaining rocks were dried for 24 h at 100 °C. The initial mass for T-03, T-05 and T-06 was 15.551 g, 14.753 g, and 158.111g, respectively. After cleaning the samples, the mass of T-03, T-05 and T-06 was 15.463 g, 14.283 g, and 156.625 g, respectively. For some tests, samples were pulverized to get basalt powder.

The samples prior CO_2 injection were characterized, under atmospheric conditions, by; 1) Petrographic microscopy using a, 2) Powder X-ray diffraction (PXRD) using a Neko QC + from Rigaku; X-ray tube: Ag anode, 4W; Detector: SDD; Environment: Air, 3) X-ray fluorescence employing a RX Bruker AX5 D8 Advance, 1°/min, potency 30 kV, 30 mA, Cu lamp, and 4) Infrared spectroscopy (IR spectroscopy) with a Bruker Alpha platinum-ATR, 12140840.

Solids before and after each experimental series were analyzed by Scanning Electron Microscopy (SEM) using a JEOL JSM-7800F Scanning Electron Microscope, Energy Dispersive X-ray Spectroscopy (EDX) was used together with SEM to identify primary and secondary minerals. When tests were run under atmospheric conditions, the pH and TDS were measured using a HANNA potentiometer, Model HI991301. While pH for high-pressure cell tests was estimated using balance matter and data from.[22]

Experimental Procedure

Carbon Dioxide Injection under Atmospheric Conditions (B1 – B3)

1. Basalt rocks (T-03, T-05 and T-06) were immersed in three different vessels with 75, 75 and, 200 mL of distilled water, respectively. The vessels were adapted to a CO_2 cylinder (99.5 % purity), using plastic tubing in direct contact with the water. The flow of CO_2 into the vessels was 1.65 L/min.
2. Three vessels were used to immersed basalt powder of T-06 (300 mg) in 40 mL of distilled water. Once again, the vessels were adapted to a CO_2 cylinder (99.5 % purity), using plastic tubing in direct contact with the water. The total exposure time of the samples to CO_2, and the water pH values for B1 to B3 are shown in the Results and Discussion Section (Table 4). As before, the flow of CO_2 into the vessels was 1.65 L/min.

Carbon Dioxide Injection under High Pressure (C1 – C3)

Basalt powder (T-06) was placed in a high-pressure cell (stainless steel), along with dry ice (CO_2) and distilled water (ice). The cell is sealed using a T-tube fitting connected to a high-pressure manometer and a safety valve. As the cell reached the room temperature, the pressure of the system increased. At this point, a heating mantle is adapted to the cell to increase the temperature, see Results and Discussion Section (Table 5).

Qualitative Analysis of Water

The determination of the total calcium and magnesium content was carried out by complexometric titration, similarly as the used to determine the total hardness of fresh water, as reported elsewhere.[23]

Results and Discussion

As shown in Table 3, the petrography analysis for the samples revealed that the most abundant mineral for the selected samples is plagioclase (with respective compositions of $NaAlSi_3O_8$ to $CaAl_2Si_2O_8$) with a mean value of 56.7 %, followed by augite (Ca, Na) (Mg, Fe, Al, Ti) $(Si, Al)_2O_6$ with a mean value of 20.8%. As it is reported, augite is an essential mineral in mafic igneous rocks, such, grabbo, basalts and ultramafic rocks. It is worth to note that sample T-06 exhibit the highest value of Augite of the selected samples for this study. Other minerals present in the samples are olivine, glass and iron oxide. Besides, none of the samples exhibit carbonates nor enstatite, which might be indicative of weathered samples. Figure 3 shows 2.5X and 10X images for T-03, T-05, and T-06 samples.

Table 3—Petrographic analysis to estimate the minerals present in the selected samples, T-03, T-05, and T-06.

Sample ID	Olivine (%)	Augite (%)	Carbonates (%)	Plagioclase (%)	Glass (%)	Iron Oxide (%)	Enstatite (%)
T-03	8	15	–	65	8	4	–
T-03'	5	15	–	70	5	5	–
T-05	8	20	–	58	6	8	–
T-05'	8	25	–	50	5	12	–

Sample ID	Olivine (%)	Augite (%)	Carbonates (%)	Plagioclase (%)	Glass (%)	Iron Oxide (%)	Enstatite (%)
T-06	8	25	–	52	3	12	–
T-06'	10	25	–	45	5	15	–

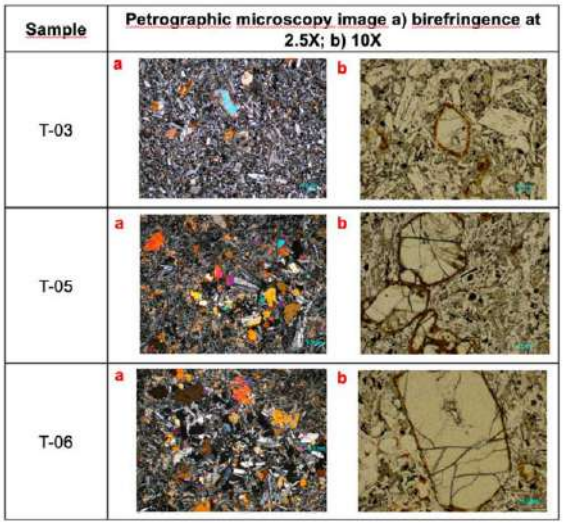

Figure 3—Petrographic microscopy images for the selected samples T-03, T-05, and T-06.

It was observed that T-03 has a Porphyritic texture, while T-05 and T-06 present Ophitic texture. The three samples are constituted mainly by a matrix in a 93 – 98% for T-03, and 85 – 90% for T-05 and T-06. The presence of crystals in the samples is low, with < 5% (, < 7% and < 8% for T-03, T-05 and T-06 respectively. Samples T-03 main phenocrysts are subhedral and euhedral pyroxenes and clinopyroxenes; sample T-05 exhibits non-aligned, iddingsitizated and subhedral olivine; sample T-06 presents high content of slightly iddingsitizated olivine phenocrysts. Samples present non or low vesicularity.

The X-ray fluorescence spectroscopy (XRF) is a non-destructive technique employed for chemical analysis, see Table 4. Taking into account the petrographic analysis (Table 3 and Figure 3) and the XRF, it is possible to confirm that the main components of the selected samples are aluminosilicates. According to the literature, the more reactive samples for CO_2 mineralization should exhibit a low content of silicates (< 50%), which confer the acidic properties of the samples. Basalts and ultramafic rocks are considered basic rocks due to the low content of silicates.[10 5] It is worth to mention that, sample T-06 is used since it presents less than 50% of aluminosilicates, this sample also exhibit a good percentage of divalent ions (Ca^{2+}, Mg^{2+}, Fe^{3+}), which are necessary for the mineralization of CO_2 into carbonates, shown as calcite ($CaCO_3$) and/or dolomite ($CaMg(CO_3)_2$).[24] Finally, the Mg uncertainty determination for T-06 is the smallest in comparison with T-03 and T-05. Therefore, sample T-06, was employed to perform most of the experiments described in the following sections.

Table 4—X-ray fluorescence (XRF) chemical analysis for samples T-03, T-05, and T-06.

Sample ID	T-03		T-05		T-06	
	Mean (%)	Uncertainty (%)	Mean (%)	Uncertainty (%)	Mean (%)	Uncertainty (%)
Si	46.13	0.072	49.653	0.2201	47.503	0.0556
Al	16.79	0.008	21.837	0.8206	12.205	0.1927
Fe	5.78	0.006	8.906	0.0042	6.683	0.0137
Mg	0.22	1.135	3.234	1.7475	4.473	0.6864

Sample ID	T-03		T-05		T-06	
Ca	6.8	0.082	7.627	0.1068	6.058	0.0093
Na	4.31	0.437	3.933	0.4733	3.824	0.8319

Once it was stablished that sample T-06 presents the most suitable properties of all the samples, we set a group of experimental conditions to estimate the reactivity of this sample with CO_2 at atmospheric and high-pressure / high-temperature conditions. The first series of experiments (B) consisted of the bubbling of CO_2 into a vessel charged with water and pulverized T-06 at atmospheric pressure and temperature. Table 5 shows the thermodynamic conditions for the 1B to 3B tests. The second series of experiments (C) consisted of the confinement of CO_2 (dry ice) with water (ice) and pulverized T-06 at high pressure and temperature. Since the solubility of CO_2 into water is highly related to pressure and temperature, we have not attempted temperatures above 50 °C. Table 5 shows the thermodynamic conditions for the 1C to 3C tests, and presents the pH values for the series B and C. In the case of the B series, pH was measured prior the CO_2 bubbling, acidity of the medium was measured periodically during the injection of carbon dioxide, however, for the sake of simplicity, only the initial and final pH values after the injection of CO_2 are presented. Due to the experimental set up for the C series, it was not possible to measure pH neither prior the CO_2 injection nor after sealing the cell. Therefore, pH value was calculated employing mass balance as well as the method reported by Diamond *et al.*[22], once the cell reached the final temperature and pressure during the first 24 h of the experiment. Final pH for the C series was determined with the potentiometer.

In general, it was observed that injection of CO_2 reduced the pH of the system considerably, due to CO_2 solubility into the aqueous medium, as CO_2 reacted or with the sample (T-06), pH values increased, and more CO_2 was injected into the system (B series). In the case of C series, it was not possible to screen the evolution of pH within the time. As shown in the next sections, we suggest that CO_2 becomes the limiting reactant, leading only to the dissolution of some ions, however, as CO_2 is consumed during this process and there is not a source of continuous carbon dioxide, mineralization is not taking place as expected.

Table 5—Experimental conditions and pH values for bubbling (1B – 3B) and high-pressure cell (1C – 3C) tests.

Sample ID	Time (min)	Temperature (°C)	Pressure (psi)	Initial pH prior CO_2 injection	Initial pH after CO_2 injection	Final pH after CO_2 injection
1B	261	25	11.31	6.00	4.63	6.19
2B	309	25	11.31	7.01	4.80	6.00
3B	540	25	11.31	7.00	5.81	8.44
1C	18,720	34	864.08	--	3.16*	5.26
2C	53,280	53	800.06	--	3.24*	7.58
3C	74,880	22	756.25	--	3.11*	8.16

*Since fluids were charged and sealed in a cell, the initial pH value was calculated using the thermodynamic parameters of the mixture using reference.[22]

After the injection of CO_2, the resulting solids were measured by powder X-ray diffraction (PXRD) to identify the main crystalline phases for the blank and the B and C series to compare the obtained products. As expected, when the CO_2 injection takes place at atmospheric conditions, the change in the PXRD patterns for the different experiments do not change, despite an increase of the time the basalt is exposed to a flow of CO_2. From the comparison between the Blank and B3, it is possible to observe that the sample is losing crystallinity, and a new phase is emerging considering the appearance of signals at 35.55°, 30.67° and 27.73° (2θ) and the disappearance of 49.73° and 51.56° (2θ)), for details see Table 6 and Figure 4. On the other hand, PXRD data for C series exhibit more significant alterations in comparison with B series, comparing

the Blank with C3, the sample with greater time of exposure to high pressure, it is possible to observe that 3C is losing crystallinity and a new phase is emerging considering the appearance of the peaks at 32.08°, 36.47° and 48.50° (2θ) as well as the fading of 27.79°, 49.78° and 51.69° (2θ)), see Table 6 and Figure 4. These results suggest that mineral phases of the samples are prone to change in the presence of CO_2. Establishing the accurate thermodynamic conditions, as well as the CO_2 injection rate are essential. Also, high pressures are needed in order to accelerate the mineralization of CO_2, and time and temperature played a critical role to assure the dissolution of CO_2 into water and set the kinetic conditions for a favorable reaction. For instance,[22] calculated that the dissolution rate of basaltic glass could be augmented by a factor of 60 by increasing the temperature from 0 to 100 °C in a solution containing 10-6 mol/kg aluminum at pH 3.5. The disadvantage with using high temperature is that the pore spaces in the host rock tend to be filled up with secondary minerals, meaning that the reactive area is low, thus, CO_2 becomes less soluble in water with increasing the temperature.

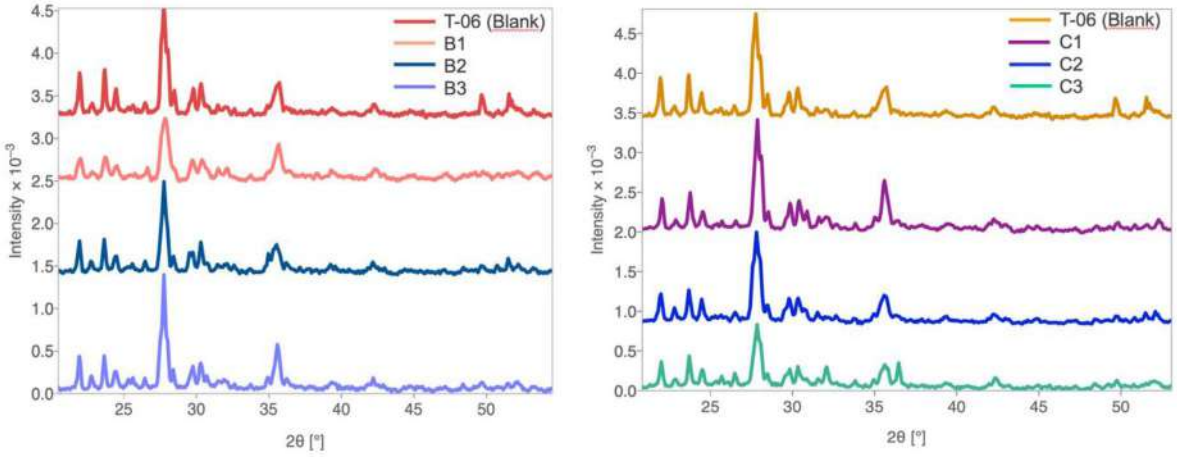

Figure 4—*Left:* Powder X-ray diffraction (PXRD) pattern for bubbling (1B – 3B) tests. T-06 (Blank) (Ca, Na)(Si, Al)$_4$O$_8$ and (CaMg$_{0.74}$Fe$_{0.25}$)Si$_2$O$_6$; 1B (CaAl$_2$Si$_2$O$_8$) and (Mg$_{0.990}$ Fe$_{0.010}$)(Ca$_{0.999}$Mg$_{0.026}$ Fe$_{0.004}$)(Si$_2$O$_6$); 2B (CaAl$_2$Si$_2$O$_8$) (Mg$_{0.990}$ Fe$_{0.010}$)(Ca$_{0.99}$ Fe$_{0.010}$) and (Ca$_{0.999}$Mg$_{0.026}$ Fe$_{0.004}$)(Si$_2$O$_6$); 3B (Mg$_{0.990}$ Fe$_{0.010}$)(Ca$_{0.999}$Mg$_{0.026}$ Fe$_{0.004}$)(Si$_2$O$_6$). *Right:* X-ray diffraction (XRD) pattern for high-pressure cell (1C – 3C) tests. 1C (Mg$_{0.990}$ Fe$_{0.010}$) (Ca$_{0.999}$Mg$_{0.026}$ Fe$_{0.004}$) (Si$_2$O$_6$); 2C Na(AlSi$_3$O$_8$) Mg$_2$SiO$_4$(Ca, Na)(Si, Al)$_4$O$_8$; 3C Na(AlSi$_3$O$_8$)Mg$_{1.787}$ Fe$_{0.213}$(SiO$_4$)CaMgSi$_2$O$_6$.

Table 6—Crystalline phases identified by powder X-ray diffraction (PXRD) for bubbling (1B – 3B) and high-pressure cell (1C – 3C) tests.

T-06 (Blank)	Sample ID	After Bubbling Test	Sample ID	After High-Pressure Cell Test
Anorthite, sodian, intermediate and Augite	1B	Anorthite Diopside ferroan	1C	Anorthite Diopside ferroan
	2B	Anorthite ordered Diopside ferroan	2C	Albite high Forsterite ferroan Northite Sodian intermediate
	3B	Diopside ferroan	3C	Albite high Forsterite ferroan

In agreement with PXRD results, the scanning electron microscopy (SEM) results showed the dissolution of divalent ions such as, Ca^{2+} and Mg^{2+}, from T-06, which produce an amorphous product, along with other ions; Na^{+}, Si^{4+}, K^{+}, Cl^{-}, S^{-}. Note that due to the natural abundance of sodium, potassium, chloride and sulphur it is not completely clear the origin of this contamination. These results suggest the feasibility of Mexican basalts to react in the presence of CO_2. After the dissolution experiments there was no visible evidence of dissolution of the basalt nor were any secondary minerals evident by this technique.

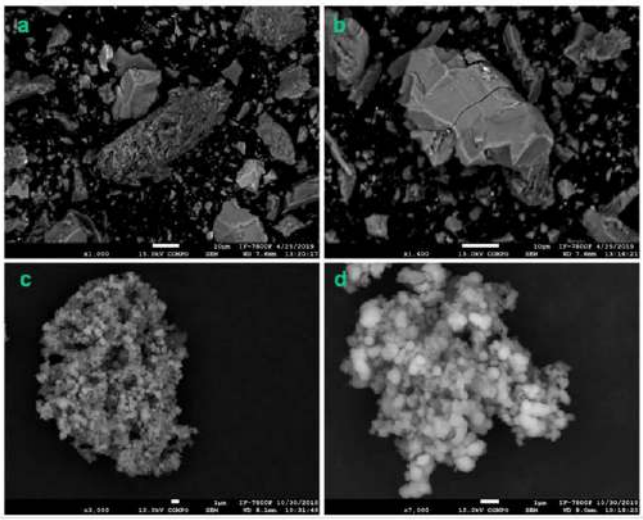

Figure 5—Scanning Electron Microscopy images of the basaltic powder for T-06 (a and b) and the minerals formed (c and d) after 1C test.

The evidence from this study suggest that CO_2 reacts with water and the carbonic acid produced releases carbonate forming cations, Ca^{2+}, Fe^{3+} and Mg^{2+}, into the solution at the same time as it consumes protons. Proton consummation increases the pH in the water, promoting the precipitation of secondary minerals, including carbonates, Table 5. The precipitation of carbonates only proceeds if the protons which are produced are being consumed by dissolution reactions like the one with basaltic glass or other common minerals in basalts, like plagioclase and Forsterite.[24]

Several methods exist to accelerate divalent cation release rates including choosing the correct type of host rock, by increasing the surface area where the mineral and fluid can react and by optimizing the composition of the injected fluid and the temperature. The accurate host rock would exhibit a high dissolution rate and high concentrations of divalent cations, like Ca^{2+}, Fe^{3+} and Mg^{2+}.[24]

Finally, the determination of the total calcium and magnesium content was carried out by complexometric titration, ant the TDS were determined as well. Preliminary results from the tests present in this study showed that the Ca^{2+} concentration for 2B, 3B, 1C, 2C, and 3C is 1.9, 6.2, 0.33, 0.24, and 0.28 μM, respectively. While Mg^{2+} concentration for 2B, 3B, 1C, 2C, and 3C is 0.79, 0.66, 4.9, 0.75 and 0.70 μM, respectively. The TDS value for tests 2B, 3B, 1C, 2C, and 3C is $3.5\times^{10-7}$, $2.7\times^{10-7}$, $2.4\times^{10-7}$, 2.8×10^{-7}, $4.2\times^{10-7}$, $1.0\times^{10-7}$, respectively. These results demonstrate the presence of divalent ions and dissolved solids after the bubbling and high-pressure cell tests; however, to have a quantitative and reliable data, it is necessary to run rigorous water analysis.

Conclusions

The mineralization of carbon dioxide, among other geological storage methods, is thought to be safest and most stable way to store this GHG. For instance, salty domes storage or exhausted reservoirs storage, those have a gas phase because of the injection, which remains buoyant from decades to hundreds of years, and consequently exists a risk of leakage to the surface. Projects such CarbFix produces carbonated minerals that are stable for millions of years, once the CO_2 is turned into minerals, the monitoring is no longer necessary.

The abundance of basaltic formations onshore is limited; however, basaltic rocks could be found also in the seabed. According to the literature, there are about eight sites onshore with plenty of igneous rocks to store CO_2, and Mexico is one of these sites. The results herein provide positive evidence for the mineralization of CO_2 using Mexican basalts, suggesting the mineral dissolution of divalent ions Ca^{2+}, Fe^{3+},

Mg^{2+}, which was confirmed by powder X-ray Diffraction (PXRD), Scanning electron microscopy (SEM) and the determination of the total calcium and magnesium content carried out by complexometric titration.

To estimate the true potential of Mexican igneous rocks, it is essential to develop more detailed cartography of the selected zones for CO_2 storage. Also, it is necessary to perform drilling activities for recovering and logging cores, as well as to develop geophysical exploration to identify the thickness and spatial distribution of basalts.

The following steps under development, consist of 1) a quantitative analysis of the water composition produced during the CO_2 injection tests; 2) the development of longer experiments, possibly using a core flood experiment for screening the transport of the fluids within the rocks. 3) combined cycle experiments involving confinement of fluids and flooding.

Acknowledgements

The authors acknowledge the support from LIRFFF group, Adriana Tejeda Cruz and Samuel Tehuacanero Cuapa, during the development of this work. ECA, POL and APGF are especially grateful with Aldo Ramos Rosique, Lino Matlalcuatzi Patiño and Andrea Salinas Hernández for fruitful discussions and support.

Acronyms

CCS – Carbon Capture and Storage
EOR – Enhanced Oil Recovery
EDX – Energy Dispersive X-ray Spectroscopy
GHG – Greenhouse Gas
Gt – Gigatons
IR – Infrared Spectroscopy
Mt – Megatons
OIB – Oceanic Island Basalts
PXRD – Powder X-ray Diffraction
SEM – Scanning Electron Microscopy
TDS – Total Dissolved Solids
TMVB – Trans-Mexican Volcanic Belt
XRF – X-ray Fluorescence

References

1. Houghton JT et al Climate Change 2001: The Scientific Basis. *Climate Change* 2001: The Scientific Basis (The Press Syndicate Of The University Of Cambridge, 2001). doi:10.1256/004316502320517344
2. Sánchez Cifuentes, A., Herrera Toledo, R. A., Moreno Coronado, T., Salas Cisneros, G. V. & Centeno Rosales, S. P. Inventario Nacional de Emisiones de Gases de Efecto Invernadero 1990-2010. *Inventario Nacional de Emisiones de Gases de Efecto Invernadero 1990-2010* **53**, (2013).
3. SENER. *Mapa de Ruta Tecnológica de CCUS en México – 2014. SENER 1*, (2014).
4. SENER. *Mapa De Ruta Tecnológica de CCUS en México - Noviembre 2018. SENER 1*, (2018).
5. Grandia, F. et al *CarbFix Final Report*. (2014).
6. Flaathen, T. K., Gislason, S. R., Oelkers, E. H. & Sveinbjörnsdóttir, Á. E. Chemical evolution of the Mt. Hekla, Iceland, groundwaters: A natural analogue for CO_2 sequestration in basaltic rocks. *Appl. Geochemistry* **24**, 463–474 (2009).

7. Oelkers, E. H. et al Using stable Mg isotope signatures to assess the fate of magnesium during the in situ mineralisation of CO_2 and H_2S at the CarbFix site in SW-Iceland. Geochim. *Cosmochim. Acta* **245**, 542–555 (2019).
8. Snæbjörnsdóttir, S. et al CO_2 storage potential of basaltic rocks in Iceland and the oceanic Ridges. *Energy Procedia* **63**, 4585–4600 (2014).
9. Snæbjörnsdóttir, S. et al The chemistry and saturation states of subsurface fluids during the in situ mineralisation of CO_2 and H_2S at the CarbFix site in SW-Iceland.*Int. J. Greenh. Gas Control* **58**, 87–102 (2017).
10. Gislason, S. R. et al Mineral sequestration of carbon dioxide in basalt: A pre-injection overview of the CarbFix project. *Int. J. Greenh. Gas Control* **4**, 537–545 (2010).
11. Ferrari, L., Orozco-Esquivel, T., Manea, V. & Manea, M. The dynamic history of the Trans-Mexican Volcanic Belt and the Mexico subduction zone. *Tectonophysics* **522–523**, 122–149 (2012).
12. Sigurdardottir, H., Gislason, S. R., Broecker, W. S., Oelkers, E. H. & Gunnlaugsson, E. *The CO_2 Fixation into Basalt at Hellisheidi Geothermal Power Plant*, Iceland. 1–4 (2010).
13. Oelkers, E. H. & Cole, D. R. Carbon dioxide sequestration: A solution to a global problem. *Elements* **4**, 305–310 (2008).
14. Global Carbon Projects. *Global Carbon Atlas. Global Carbon Atlas* (2018). Available at: http://www.globalcarbonatlas.org/en/CO2-emissions.
15. Oelkers, E. H., Gislason, S. R. & Matter, J. Mineral carbonation of CO_2.*Elements* **4**, 333–337 (2008).
16. Gómez Tuena, A., Orozco Esquivel, M. T., Ferrari, L. & et al Petrogénesis ígnea de la faja Volcánica Transmexicana. *Boletín la Soc. Geológica Mex. LVII*, 227–283 (2005).
17. Ferrari, L. Avances en el Conocimiento de la Faja Volcánica Transmexicana Durante la Última Década. *Boletín la Soc. Geológica Mex*. **LIII**, 84–92 (2000).
18. Mori, L., Gómez-Tuena, A., Schaaf, S. G., Pérez-Arvizú, O. & Solís-Pichardo, G. *Lithospheric Removal as a Trigger For Flood Basalt Magmatism In The Trans-Mexican Volcanic Belt. J. Petrol. LII*, 2157–2186 (2009).
19. World Resources Institute. *Water Stress by Country*. (2013). Available at: https://www.wri.org/resources/charts-graphs/water-stress-country.
20. Beltrán, L. et al *Atlas de Almacenamiento Geológico de CO_2 - México*. (2012).
21. Ferrari, L., Orozco Esquivel, T., Navarro, M., López-Quiroz, P. & Luna, L. Digital Geologic Cartography and Geochronologic Database of the Trans-Mexican Volcanic Belt and Adjoining Areas. *Terra Digit*. **2**, 1–8 (2018).
22. Diamond, L. W. & Akinfiev, N. N. Solubility of CO_2 in water from −1.5 to 100°C and from 0.1 to 100 MPa: Evaluation of literature data and thermodynamic modelling. *Fluid Phase Equilib*. **208**, 265–290 (2003).
23. University Of Canterbury. *Determination Of Total Calcium and Magnesium Ion Concentration*. **3** (2011).
24. Flaathen, T. K. *WATER-ROCK INTERACTION DURING CO_2 SEQUESTRATION IN BASALT Dissertation for the Degree of Doctor of Philosophy Water-Rock Interaction During CO_2 Sequestration in Basalt (Étude de l ' Interaction Eau-Basaltes Lors d ' Injection de CO_2)*. (2009).